Involvement of the ATR- and ATM-Dependent Checkpoint Responses in Cell Cycle Arrest Evoked by Pierisin-1

Bunsyo Shiotani,[1] Masahiko Kobayashi,[2] Masahiko Watanabe,[1] Ken-ichi Yamamoto,[2] Takashi Sugimura,[1] and Keiji Wakabayashi[1]

[1]Cancer Prevention Basic Research Project, National Cancer Center Research Institute, Tokyo, Japan and [2]Department of Molecular Pathology, Cancer Research Institute, Kanazawa University, Kanazawa, Japan

Abstract

Pierisin-1 identified from the cabbage butterfly, *Pieris rapae*, is a novel mono-ADP-ribosylating toxin that transfers the ADP-ribose moiety of NAD at N^2 of dG in DNA. Resulting mono-ADP-ribosylated DNA adducts cause mutations and the induction of apoptosis. However, little is known about checkpoint responses elicited in mammalian cells by the formation of such bulky DNA adducts. In the present study, it was shown that DNA polymerases were blocked at the specific site of mono-ADP-ribosylated dG, which might lead to the replication stress. Pierisin-1 treatment of HeLa cells was found to induce an intra-S-phase arrest through both ataxia telangiectasia mutated (ATM) and Rad3-related (ATR) and ATM pathways, and ATR pathway also contributes to a G_2-M-phase delay. In the colony survival assays, *Rad17*$^{-/-}$ DT40 cells showed greater sensitivity to pierisin-1-induced cytotoxicity than wild-type and *ATM*$^{-/-}$ DT40 cells, possibly due to defects of checkpoint responses, such as the Chk1 activation. Furthermore, apoptotic 50-kb DNA fragmentation was observed in the HeLa cells, which was well correlated with occurrence of phosphorylation of Chk2. These results thus suggest that pierisin-1 treatment primarily activates ATR pathway and eventually activates ATM pathway as a result of the induction of apoptosis. From these findings, it is suggested that mono-ADP-ribosylation of DNA causes a specific type of fork blockage that induces checkpoint activation and signaling. (Mol Cancer Res 2006;4(2):125–33)

Introduction

Pierisin-1 is a novel apoptosis-inducing protein identified from cabbage butterfly, *Pieris rapae* (1-3). The cytotoxic potency of pierisin-1 varies among different cell lines, with IC_{50}s ranging from 0.043 to 270 ng/mL in 13 cell lines tested (4, 5). Pierisin-1 is an ADP-ribosylating toxin targeting a DNA rather than proteins (6), and the protein consists of a NH_2-terminal ADP-ribosyltransferase enzymatic domain, which catalyzes the transfer of ADP-ribose moieties from NAD to guanine residues of DNA, and a COOH-terminal receptor-binding domain, which is responsible for incorporation into cells by binding to glycosphingolipid receptors (5, 7, 8). The chemical structures of mono-ADP-ribosylated dG are concluded to be N^2-(α-ADP-ribos-1-yl)-2′-dG and its β-form (8, 9). The guanine adducts produced can lead to mutations in the *HPRT* and *supF* genes (10), and the system responsible for repair of mono-ADP-ribosylated dG adducts due to pierisin-1 involves nucleotide excision repair (11). In addition, pierisin-1 induces apoptosis via the mitochondrial pathway that can be blocked by the overexpression of Bcl-2 (12). The mono-ADP-ribosylated dG produced by pierisin-1, therefore, might associate with the induction of apoptosis and mutations.

In response to DNA damage, checkpoint signals are evoked primarily in the form of kinase-mediated protein phosphorylation to arrest cells in the G_1-S, S, and G_2-M phases and allows time for repair to take place (13). Ataxia telangiectasia mutated (ATM) and/or ATM-Rad3-related (ATR) kinases are activated, are dependent on DNA damage, and phosphorylate downstream effector kinases, such as Chk1 and Chk2. Whereas ATM seems to be activated mainly by ionizing radiation (IR)–induced DNA DSBs, ATR acts in response to a variety of DNA-damaging agents, including UV irradiation. Thus, these kinases relay and amplify the damage signal and effector proteins that control cell cycle progression, chromatin restructuring, and DNA repair. DNA damage–induced checkpoint response has been studied extensively in many laboratories but mainly in context of UV- or IR-induced alteration (14, 15). In contrast, little is known regarding molecular mechanisms of checkpoint responses elicited in mammalian cells by other form of DNA damage, such as bulky adducts.

Some carcinogens are known to form bulky DNA adducts, such as 2-acetylaminofluorene, which generates guanine adducts at C-8 (16) resulting in replication stress through inhibition of DNA polymerases and then activates ATR (17). Under conditions of replication stress, ATR mainly activates downstream target Chk1 in a Rad17-dependent manner (18). The contribution of Chk1 in the S- and G_2-M-phase checkpoint is well understood to be mediated by phosphorylation of Cdc25A and Cdc25C, respectively (14). A recent study provided evidence of the existence of a caffeine-sensitive,

Received 7/20/05; revised 1/10/06; accepted 1/19/06.
Grant support: Ministry of Health, Labor and Welfare of Japan Grant-in-Aid for Cancer Research; Foundation for Promotion of Cancer Research resident fellowship (B. Shiotani).
The costs of publication of this article were defrayed in part by the payment of page charges. This article must therefore be hereby marked advertisement in accordance with 18 U.S.C. Section 1734 solely to indicate this fact.
Requests for reprints: Keiji Wakabayashi, Cancer Prevention Basic Research Project, National Cancer Center Research Institute, 5-1-1 Tsukiji, Chuo-ku, Tokyo 104-0045, Japan. Phone: 81-3-3542-2511; Fax: 81-3-3543-9305. E-mail: kwakabay@gan2.res.ncc.go.jp

doi:10.1158/1541-7786.MCR-05-0104

Chk1-mediated, S-phase arrest that is operational in response to benzo(*a*)pyrene dihydrodiol epoxides (19). Benzo(*a*)pyrene dihydrodiol epoxides bind covalently to the N^2 position of dG, the location of mono-ADP-ribosylation by pierisin-1.

Given the essential role of ATR and ATM in genome maintenance, in the present study, we focused on the checkpoint signals in response to mono-ADP-ribosylated dG produced by pierisin-1. Our results indicate that the replication stress caused by the inhibition of polymerase may activate the checkpoint responses mediated by ATR-Rad17-Chk1 leading to cell cycle arrest at S and G_2-M phases. ATM-Chk2 and Chk2 pathways are also activated possibly due to the production of characteristic 50-kb DNA fragments in pierisin-1-treated cells and may partially contribute to S-phase arrest. The importance of mono-ADP-ribosylated dG for the activation of checkpoint responses is discussed.

Results

Effect of ADP-Ribosylated dG on DNA Replication

Primer extension assays using pierisin-1-modified and unmodified oligonucleotides as templates showed blocking potential of the ADP-ribosylated dG adduct on replication by polymerase α, β, and I (Fig. 1A). Replication of unmodified DNA templates by the family B polymerases, polymerases α and I, was highly efficient, with full extension products within 5 minutes of initiation of reaction. For family X polymerase β, the extension reaction was almost completed within 30 minutes. In contrast, replication of pierisin-1-modified templates with each polymerase was completely blocked one base before the ADP-ribosylated dG. Crude extracts from HeLa cells were also efficient in extension reaction of unmodified templates, and the extension reaction was partially inhibited by a polymerase α–selective inhibitor aphidicolin (Fig. 1B). Replication of pierisin-1-modified templates by crude extracts was blocked one base before the modified dG, and the extension reaction was inhibited by aphidicolin. Moreover, aphidicolin inhibited only polymerase α but not polymerase β. These results indicate that the ADP-ribosylated dG adducts block primer extension by polymerases leading to replication stress.

S-Phase Arrest and G2-M-Phase Delay Induced by Pierisin-1 in HeLa Cells

To investigate the effect of pierisin-1 on the cell cycle, HeLa/Bcl-2 cells were synchronized at the G_1-S boundary by a thymidine block method. Figure 2 shows representative cell cycle profiles of HeLa/Bcl-2 cells treated with or without 1,000 pg/mL pierisin-1. The experiment was repeated on more than three separate occasions with similar results. The cells were accumulated in the middle S phase at 4 hours later of pierisin-1 treatment, and the cell cycle profile was almost same until 24 hours after treatment, when they were treated with pierisin-1 for 1 hour just after the release of the thymidine block (Fig. 2A). In addition, the cell cycle progression through the G_2-M phase was delayed compared with the nontreatment case, when the cells were treated with pierisin-1 for 1 hour after 6 hours late of the release (Fig. 2B), and the cells seemed to be arrested in the next G_1 phase at 24 hours. It is possible that they might be

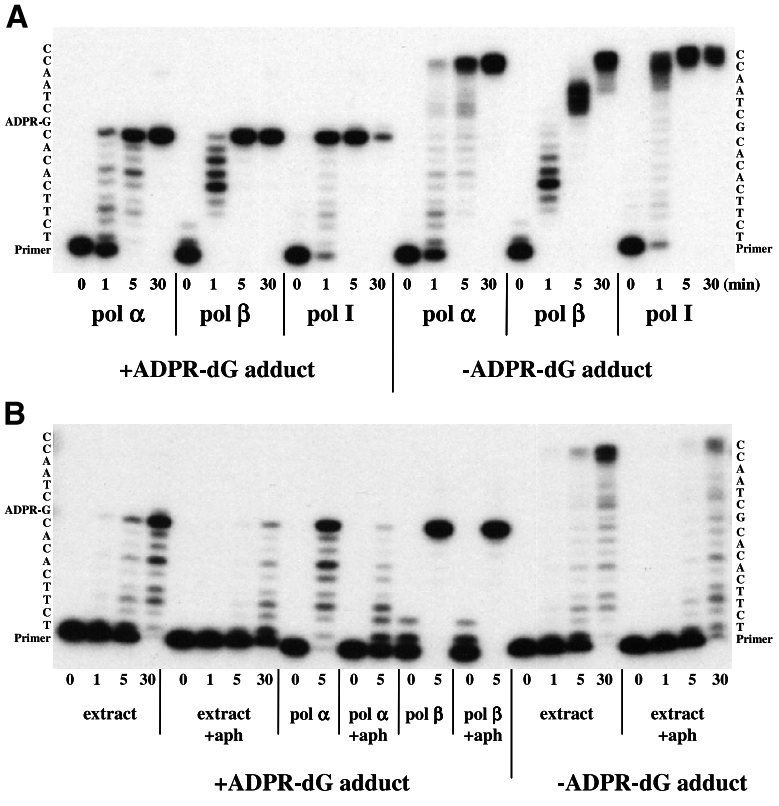

FIGURE 1. Effects of ADP-ribosylated dG on DNA replication. After annealing the 30-base oligonucleotide, either ADP-ribosylated or unmodified, with the 14-base primer, the annealed DNA was incubated for indicated time (minutes) with mammalian polymerase (*pol*) α and β and *E. coli* polymerase I (**A**) or HeLa cytosol (**B**). To inhibit DNA polymerase α, 10 μg/mL aphidicolin was included in the reaction mixture. Reactions were terminated by addition of gel loading buffer containing formamide, and extension products were separated on 15% denaturing polyacrylamide gel and subjected for autoradiography.

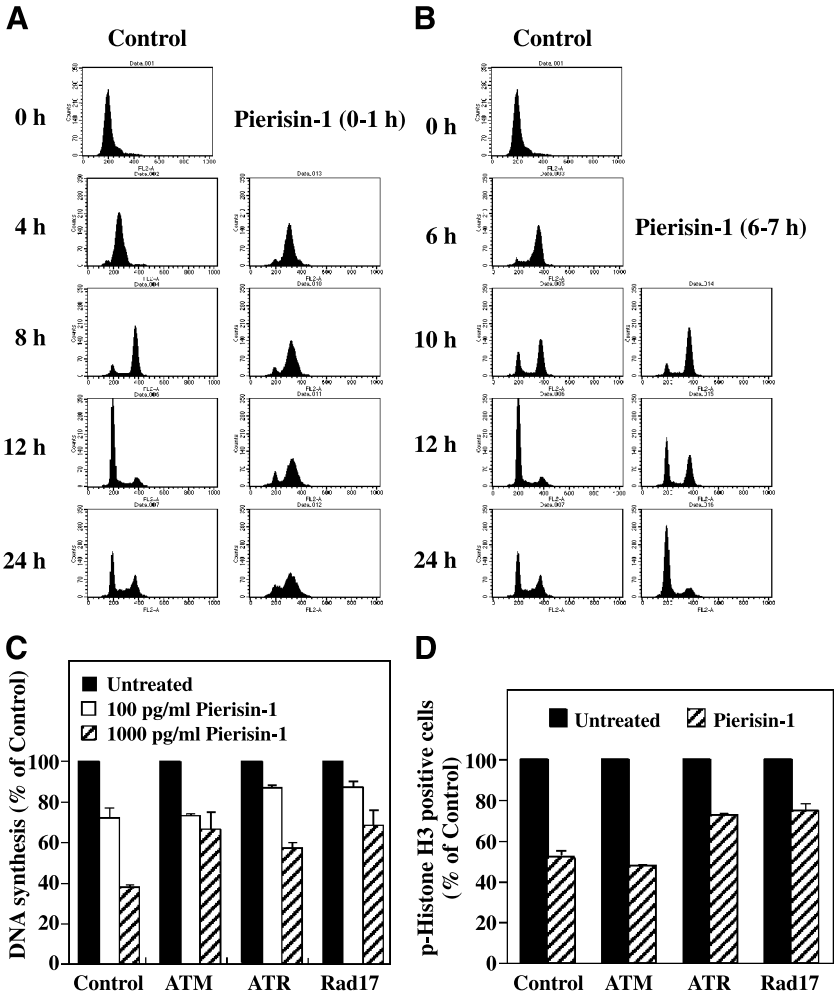

FIGURE 2. S-phase arrest and G_2-M-phase delay induced by pierisin-1. For cell cycle distribution analysis, HeLa/Bcl-2 cells were synchronized at G_1-S phase by the double thymidine block method. These cells were treated with 1,000 pg/mL pierisin-1 for 1 hour just after the release (**A**) or 6 hours after the release from the thymidine block (**B**), harvested at the indicated time point, and analyzed by the flow cytometry as described in Materials and Methods. Fluorescence data were displayed as peaks using the CellQuest software. **C.** Asynchronized HeLa cells were transfected with siRNAs for control, ATM, ATR, and Rad17 as described in Materials and Methods and treated with 100 and 1,000 pg/mL pierisin-1 for 6 hours. Rates of DNA synthesis of resulting cultures were determined by [^{3}H]thymidine incorporation. Columns, mean of at least three separate experiments; bars, SD. **D.** Cultures with the indicated siRNA were transfected as described in (**C**) and incubated with nocodazole for 8 hours with or without treatment with 1,000 pg/mL with pierisin-1. Percentages of phosphorylated histone H3–positive cells were determined. Columns, mean of at least three separate experiments; bars, SD.

arrested in the very early S phase, because sufficient amounts of DNA adducts could already be formed during the 6- to 10-hour cultivation, and p53, which is a main regulator of G_1 arrest, is inactive in HeLa cells.

To determine if pierisin-1-induced S-phase arrest is dependent on checkpoint responses, DNA synthesis was assessed in asynchronized HeLa cells 6 hours after pierisin-1 treatment. In cells transfected with nonsilencing control small interfering RNA (siRNA), 100 and 1,000 pg/mL pierisin-1 treatment reduced DNA synthesis to 72% and 32% of that in untreated cells, respectively (Fig. 2C). Whereas inhibition of DNA synthesis induced by 100 pg/mL pierisin-1 was restored in the ATR and Rad17 knockdown cells but not in ATM knockdown cells, that induced by 1,000 pg/mL pierisin-1 was restored in ATM, ATR, and Rad17 knockdown cells. Moreover, the knockdown effects of ATM, ATR, and Rad17 on the mitotic delay were examined by quantifying cells containing phosphorylated histone H3. Pierisin-1 treatment (1,000 pg/mL) reduced histone H3 phosphorylation in asynchronized HeLa cells by 47% compared with the untreated control (Fig. 2D). ATM knockdown did not significantly affect the G_2-M delay induced by pierisin-1. On the other hand, knockdown of ATR and Rad17 partially deviated this delay. These results suggest that, in addition to the physiologic inhibition of the replication apparatus by the DNA adduct itself, ADP-ribosylated dG induced by pierisin-1 activated intra-S-phase and G_2-M checkpoint through ATR-Rad17 pathway. In cells treated by high dose of pierisin-1, ATM pathway also contributes to intra-S-phase checkpoint response.

Checkpoint Responses to Pierisin-1 in Rad17$^{-/-}$ and ATM$^{-/-}$ DT40 Cells

To investigate which checkpoint responses might be involved for cell survival, a survival assay and a mitotic entry assay using *Rad17*$^{-/-}$ and *ATM*$^{-/-}$ DT40 cells were conducted (Fig. 3A and B). Because the cytotoxic potency of pierisin-1 largely varies in cell lines, DT40 cells were treated with higher doses of pierisin-1. Cytotoxicity assay of pierisin-1 assessed by WST-1 methods showed that IC_{50}s at 24 hours were 400 ng/mL for DT40 cells and 500 pg/mL for HeLa cells (data not shown).

Pierisin-1 exerted a much greater antiproliferative effect on *Rad17*$^{-/-}$ cells than on their wild-type or ATM$^{-/-}$ counterparts, suggesting that Rad17- but not ATM-related checkpoint pathways might contribute to the cell survival that might be

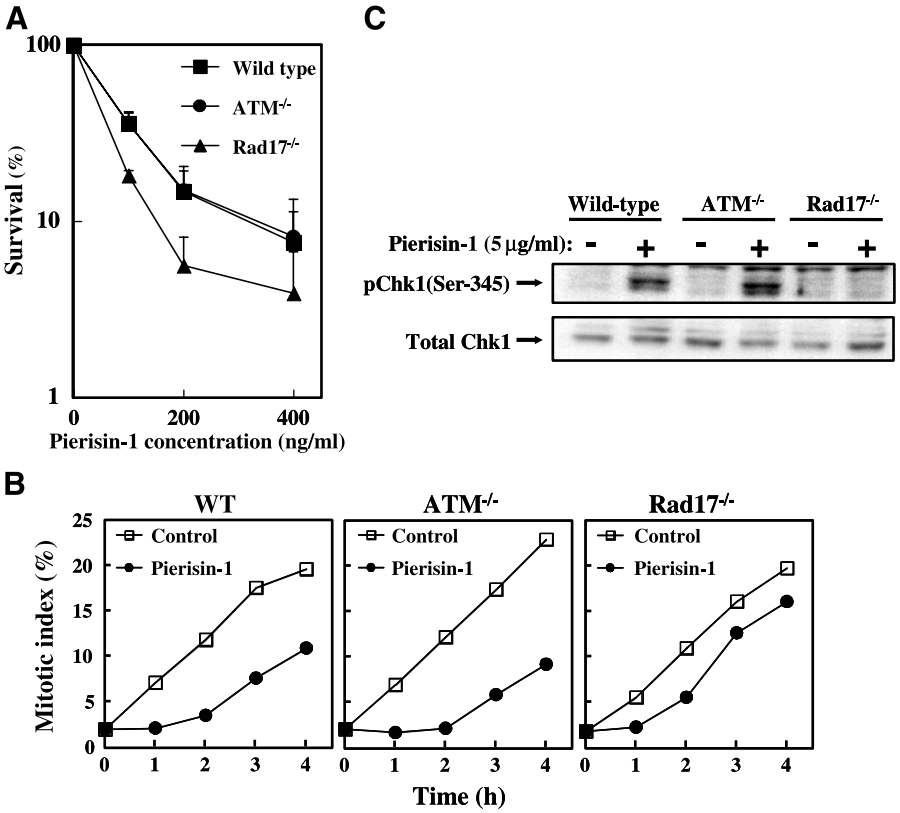

FIGURE 3. Increased sensitivity of *Rad17*$^{-/-}$ DT40 cells to pierisin-1. **A.** Clonogenic survival of indicated clones following pierisin-1 treatment at the indicated concentration for 4 hours. Points, mean of at least three separate experiments per clone; bars, SD. **B.** Each culture untreated or treated with 5 μg/mL pierisin-1 was incubated with nocodazole for indicated time, and percentages of phosphorylated histone H3–positive cells were determined. The experiment was repeated on more than three separate occasions with similar results. **C.** Cells were harvested after treatment with 5 μg/mL pierisin-1 for 3 hours. Equal amounts of proteins were subjected to Western blot detection of total Chk1 and phospho-Chk1 (Ser^{345}).

threatened by ADP-ribosylated dG produced by pierisin-1. Although the influence of pierisin-1 on cell cycle distribution was analyzed as for HeLa cells, toxic effects of thymidine on DT40 cells were too severe to allow assessment of S-phase accumulation (data not shown). Therefore, G_2-M checkpoint responses to the pierisin-1 treatment were further analyzed using mitotic entry analysis (Fig. 3B). Although pierisin-1-induced mitotic delay was clearly detectable in wild-type and *ATM*$^{-/-}$ cells, it was not observed in *Rad17*$^{-/-}$ cells, showing that Rad17 is required for the pierisin-1-induced checkpoint responses. Because Chk1 plays an essential role in the replication checkpoint control and Rad17 is required for Chk1 activation induced by genotoxic agents, we assessed whether Chk1 activation might be involved in the pierisin-1-induced checkpoint responses (18). Treatment of wild-type and *ATM*$^{-/-}$ cells with pierisin-1 led to activation of Chk1 as evidenced by increased phosphorylation of Ser^{345} (Fig. 3C). In contrast, activation of Chk1 was not observed in *Rad17*$^{-/-}$ DT40 cells, indicating that pierisin-1 induced Rad17- and Chk1-mediated G_2-M checkpoint responses in DT40 cells.

Checkpoint Responses Induced by Pierisin-1 in HeLa Cells

It has been reported that the ATR-Chk1 pathway can respond not only to DSBs but also to agents that interfere function of DNA replication forks, such as UV and hydroxyurea, whereas ATM-Chk2 checkpoint pathway responds to the presence of DSBs. For further investigation of checkpoint responses induced by pierisin-1 in HeLa cells, activation of Chk1 and Chk2 as a result of phosphorylation by upstream kinases ATR and ATM was assessed. Activation of Chk2 was analyzed by using the commercially available phosphospecific antiserum, which recognizes phospho-Thr^{68} of Chk2. Activated Chk1 and Chk2 were observed after 6-hour treatment with pierisin-1 (Fig. 4A). Hydroxyurea, which is generally used as the inducer of replication stress, activated Chk1 but not Chk2 after 2- and 4-hour treatment at 2 mmol/L. Activation of ATM assessed with a phosphospecific monoclonal antibody, which recognizes phospho-Ser^{1981} of ATM, was observed 2 hours after pierisin-1 treatment, and the cleaved form of ATM, which was suggested to be a result of apoptosis (20), was detected at 9 and 12 hours. Furthermore, phosphorylation of histone H2AX (DSB marker) was slightly detected at 6 hours and immensely at 9 and 12 hours. After 6-hour treatment with various concentrations, activation of Chk1 and Chk2 was increased in a dose-dependent manner (Fig. 4B). Activation of ATM was also increased at 50 pg/mL pierisin-1, although phosphorylation of histone H2AX was barely detected at this time point (Fig. 4A and B). To investigate the requirement of upstream kinases for the activation of Chk1 and Chk2 after 6-hour treatment of pierisin-1, siRNAs specifically inhibit expression of ATM, ATR, and Rad17 in HeLa cells. Introduction of ATM, ATR, and Rad17 targeting siRNA duplexes led to significant decreases in the respective protein levels, respectively (Fig. 5A). Chk1 activation was totally abrogated in ATR knockdown cells and partially diminished in Rad17 knockdown cells. These results suggest that ATR-Rad17-Chk1-mediated checkpoint responses might also occur in pierisin-1-treated HeLa cells. On the other

hand, Chk2 activation was only slightly decreased in ATM knockdown cells. To clarify whether Chk2 activation by pierisin-1 treatment might be caused without ATM, an ATM-deficient fibroblast line, AT22IJE-T cells (ATM-deficient), in which *ATM* gene is mutated, and the ATM-deficient cells complemented with *ATM* minigene (pEBS7-YZ5) were used (21). Chk2 activation induced by pierisin-1 was clearly observed even in the ATM-deficient cells, whereas activation of Chk2 by IR was observed only in the ATM-complemented cells, suggesting that mono-ADP-ribosylated dG produced by pierisin-1 might cause activation of Chk2 in both ATM-dependent and ATM-independent manners (Fig. 5B).

Large-Scale DNA Fragmentation (50 kb) Induced by Pierisin-1 in HeLa Cells

To confirm whether DSBs occur in pierisin-1-treated HeLa cells, genomic DNA was analyzed by the pulsed-field gel electrophoresis (PFGE) method. Large-scale DNA fragmentation (~50 kb), different from γ-ray and etoposide exposure, occurred in a time- and dose-dependent manner (Fig. 6A and B), being increased after 6-hour treatment with 1,000 pg/mL pierisin-1. The lowest concentration of pierisin-1 leading to large-scale DNA fragmentation was 50 pg/mL, consistent with the concentration required to ATM activation (see Fig. 4B).

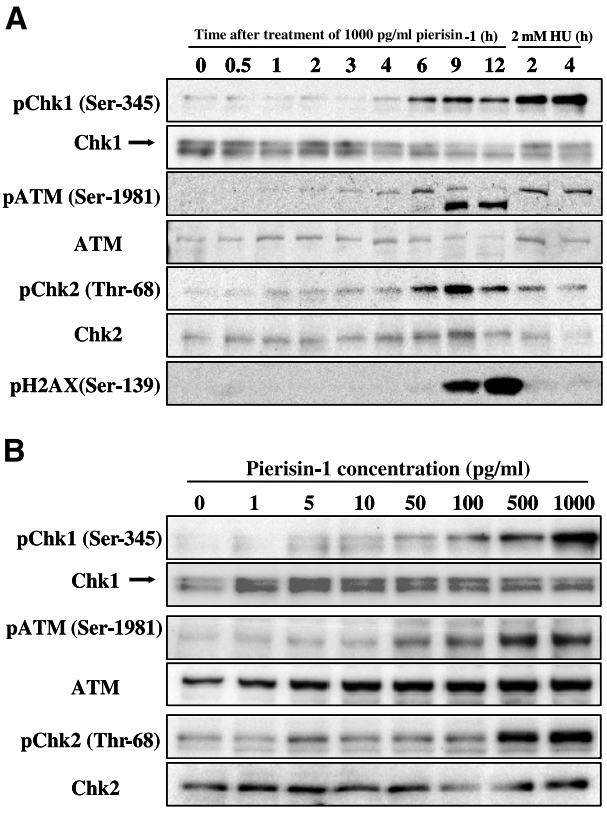

FIGURE 4. Activation of Chk1, Chk2, and ATM by pierisin-1 treatment in HeLa cells. HeLa cells were harvested after treatment with 1,000 pg/mL pierisin-1 for the indicated times (**A**) after exposure to various concentrations of pierisin-1 for 6 hours (**B**). Equal amounts of proteins were subjected to Western blot detection of total Chk1, Chk2, ATM and phospho-Chk1 (Ser^{345}), phospho-Chk2 (Thr^{68}), phospho-ATM (Ser^{1981}), and phosphorylated histone H2AX.

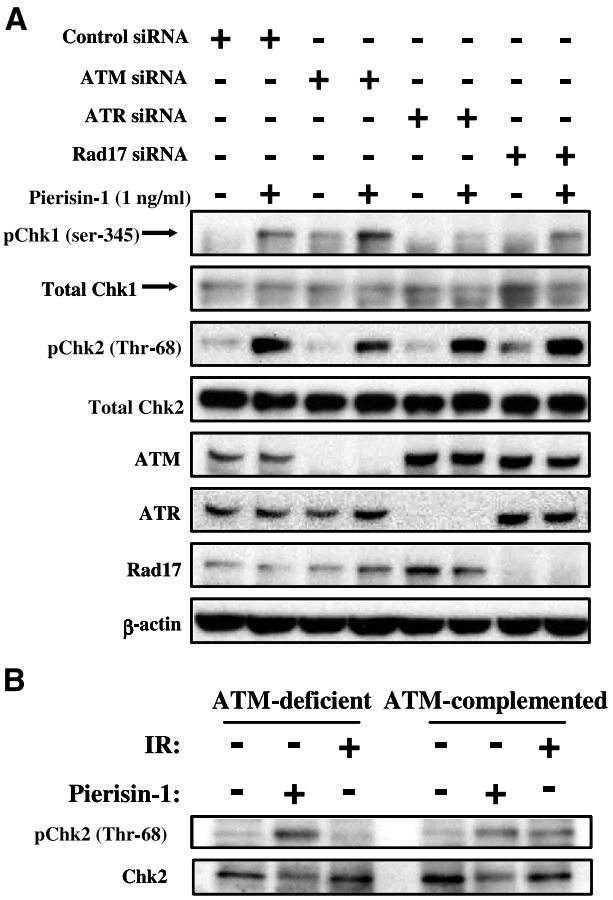

FIGURE 5. Defects of checkpoint responses induced by pierisin-1 in ATR and Rad17 knockdown HeLa cells. **A.** HeLa cells were transfected with siRNAs for control, ATM, ATR, and Rad17 as described in Materials and Methods and harvested after treatment with 1,000 pg/mL pierisin-1 for 6 hours. Equal amounts of proteins were subjected to Western blot detection of total Chk1, Chk2, ATM, ATR, Rad17, phospho-Chk1 (Ser^{345}), and phospho-Chk2 (Thr^{68}). Western blot for actin was used as the lording control. **B.** ATM-deficient fibroblasts AT22IJE-T and the matched line complemented with ATM minigene (ATM-deficient + ATM) were harvested after treatment with 10 ng/mL pierisin-1 for 24 hours or after 30-minute cultivation following IR (10 Gy). Equal amounts of proteins were subjected to Western blot detection of total Chk2 and phospho-Chk2 (Thr^{68}).

These DNA fragmentations were not observed in the 2 mmol/L hydroxyurea-treated cells (Fig. 6A). It has been reported that the 50-kb fragment was generated during apoptosis mediated by the apoptosis-inducing factor, which is a mitochondrial effector of apoptotic cell death (22). Overexpression of Bcl-2, which controls the opening of mitochondrial permeability transition pores, impeded the pierisin-1-induced DNA fragmentation but not that induced by *N*-methyl-*N*′-nitro-*N*-nitrosoguanidine, which directly induces mitochondrial permeability transition (Fig. 7A). In addition, ATM and Chk2 activation was largely reduced in HeLa/Bcl-2 cells (Fig. 7B). These results suggest that ATM can be activated by apoptotic large-scale DNA fragmentation induced by pierisin-1.

Discussion

Pierisin-1 is a novel mono-ADP-ribosylating protein, which induces apoptosis and mutations to mammalian cells. These

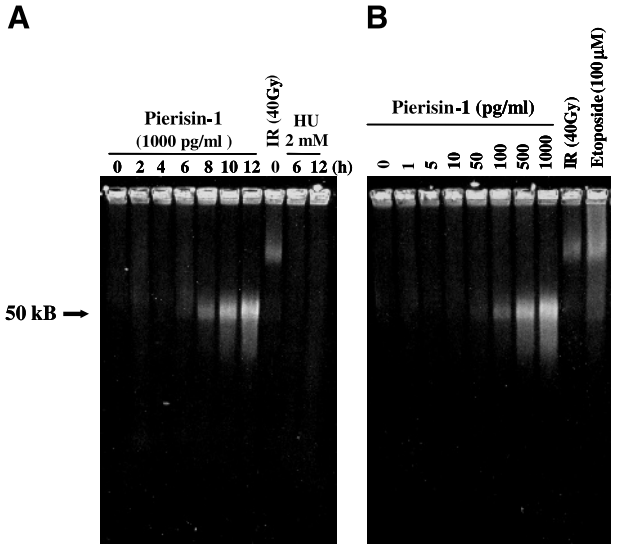

FIGURE 6. Large-scale DNA fragmentation (50 kb) induced by pierisin-1 in HeLa cells. HeLa cells were harvested after treatment with 1,000 pg/mL pierisin-1 or 2 mmol/L hydroxyurea (*HU*) for indicated times or after 0 hour following IR (40 Gy) exposure (**A**) and after treatment with various concentrations of pierisin-1 or 100 μmol/L etoposide for 12 hours or after 0 hour following IR (40 Gy) exposure (**B**). Cells were subjected to PFGE to visualize ~50-kb DNA fragments as described in Materials and Methods. Similar results were obtained in three independent experiments.

actions might be triggered by formation of mono-ADP-ribosylated dG catalyzed by pierisin-1, and in the present study, we obtained evidence of polymerase inhibition leading to replication stress involving the ATR-Rad17-Chk1 checkpoint pathway that might contribute to S-phase arrest and G_2-M-phase delay. In addition, we found that pierisin-1 induced large-scale DNA fragmentation that likely lead to activation of ATM-Chk2 pathway. Thus, it is suggested that pierisin-1 induces dual checkpoint responses mediated not only by ATR but also by ATM.

Bulky DNA adducts generally interfere with the DNA replication apparatus leading to replication stress. At the sites of stalled replication forks, ssDNA is generated and coated by replication protein A, a ssDNA-binding protein complex (23), which is required for the recruitment of ATR-ATR-interacting protein complex to sites of DNA damage (24). In addition, replication protein A mediates recruitment and activation of the Rad17 complex, which is a replication factor C–like protein complex in which Rfc1 is substituted by Rad17 (25). Although the localization of ATR and Rad17 are largely independent, they function in concert to fully activate the damage response, including Chk1 phosphorylation, mediated by Rad9-Rad1-Hus1 complex (18, 26). The present study showed that mono-ADP-ribosylated dG produced by pierisin-1 blocks replication by polymerases, thus directly causing S-phase arrest. In addition, replication stress caused by the inhibition of replication triggered ATR-Rad17-Chk1-mediated checkpoint responses, so that cells became arrested in both S and G_2-M phases. Surprisingly, large-scale DNA fragmentation, which has been reported with apoptosis mediated by apoptosis-inducing factor, occurred after treatment with pierisin-1 and clearly differed from DSBs induced by IR and etoposide. Although robust activation of ATM pathway correlated the occurrence of large-scale DNA fragmentation, weak activation of ATM was observed in the absence of detectable DSBs assessed by PFGE in the pierisin-1-treated HeLa/Bcl-2 cells, suggesting that mono-ADP-ribosylation of amino group at N^2 position of dG might result in disruption of the double-helix structure of genomic DNA, because this position is critical for formation of hydrogen bonds with dC. The results support the hypothesis that ATM might sense and respond to changes in chromatin structure in response to cellular irradiation but not direct binding to DSBs (27). Thus, ATM might be even activated by the topological changes of DNA caused by the production of DNA adducts, and such activation was accelerated by the large-scale DNA fragmentation.

The roles of Chk2 in the checkpoint response are complicated. It has been determined previously that Chk2 regulates G_1- and S-phase arrest when DSBs are present (14), but phenotypic analysis of *Chk2*$^{-/-}$ murine fibroblasts revealed only subtle or no defects in the G_1- and S-phase checkpoints (28-30). However, apoptosis defects have been shown in Chk2-deficient mice (31). After treatment with

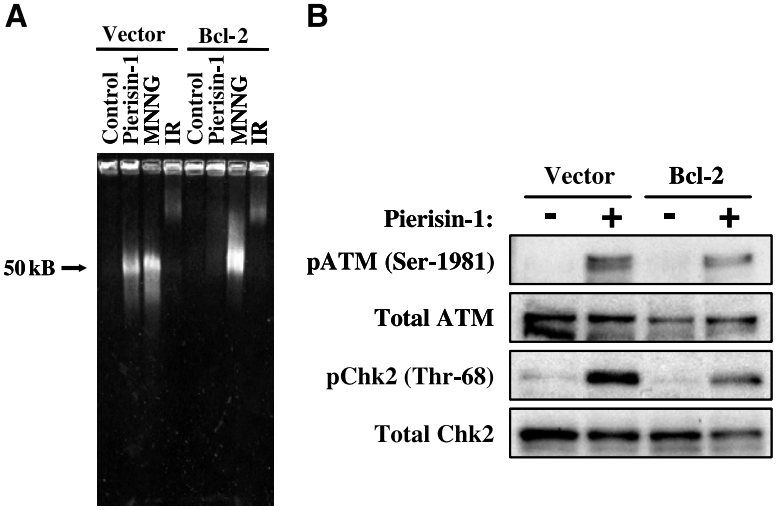

FIGURE 7. Large-scale DNA fragmentation-independent ATM and Chk2 activation induced by pierisin-1. **A.** HeLa cells transfected with a Bcl-2 expression vector (*Bcl-2*) or a control vector (*Vector*) were treated with or without 1,000 pg/mL pierisin-1 for 12 hours or cultured for 12 hours following 0.5 mmol/L *N*-methyl-*N*′-nitro-*N*-nitrosoguanidine (*MNNG*) treatment for 15 minutes or cultured for (6) 0 hour following IR (40 Gy) exposure. Cells were subjected to PFGE to visualize ~50-kb DNA fragment as described in Materials and Methods. Similar results were obtained in three independent experiments. **B.** HeLa cells transfected with a Bcl-2 expression vector or a control vector were harvested after treatment with 1,000 pg/mL pierisin-1 for 6 hours or cultured for 6 hours following 0.5 mmol/L *N*-methyl-*N*′-nitro-*N*-nitrosoguanidine for 15 minutes. Equal amounts of proteins were subjected to Western blot detection of total ATM, phospho-ATM (Ser^{1981}), Chk2, and phospho-Chk2 (Thr^{68}).

pierisin-1 at concentrations sufficient to induce apoptosis, Chk2 was activated in HeLa cells and this was reduced by Bcl-2 overexpression, suggesting that Chk2 may have a partial role in the pierisin-1-induced apoptosis. In addition, Chk2 was activated in ATM-deficient cells, indicating that Chk2 might be activated in a ATM-independent manner. Recent reports indicate that polo-like kinase family members, including Plk1, and TTK/hMps1 that regulate many critical events in mitosis may be involved in the phosphorylation of Chk2 (32-34). It remains to be elucidated whether the formation of mono-ADP-ribosylation of dG perturbs mitotic events and activates the spindle assembly checkpoint.

Pierisin-1 induces caspase-dependent apoptosis via mitochondrial pathway that can be blocked by Bcl-2 (12). Mitochondrial proteins that cause caspase-dependent apoptosis include cytochrome *c*, which triggers caspase-9 activation by binding, activating the apoptosis protease-activating factor-1, and many other proteins regulating the activation of caspase (35). Mitochondria have also been reported to contain the caspase-independent death effector apoptosis-inducing factor, which induces chromatin condensation and large-scale DNA fragmentation (50 kb) when translocated into the nucleus (22). It has been reported that apoptosis-inducing factor–mediated apoptosis induced by alkylating agent *N*-methyl-*N*′-nitro-*N*-nitrosoguanidine is dependent on poly(ADP-ribose) polymerase-1, which is an enzyme, similar to pierisin-1, consuming a NAD as a substrate (36). Poly(ADP-ribose) polymerase-1 is activated in response to DNA damage and forms ADP-ribose polymers using NAD. The resultant NAD depletion can cause glycolytic failure and lead to poly(ADP-ribose) polymerase-1–dependent apoptosis (37), although we here found no major change in cellular NAD levels after treatment pierisin-1 (data not shown). Our present study showed pierisin-1 to induce large-scale DNA fragmentation, which might be mediated by apoptosis-inducing factor, but exact mechanisms remain to be elucidated.

In summary, pierisin-1, a novel ADP-ribosylating protein, activates DNA damage signaling pathways, including the ATR-Rad17-Chk1 through replication stress caused by inhibition of polymerases at the mono-ADP-ribosylated dG, with consequent cell cycle arrest. The ATM-Chk2 pathway is also activated possibly due to the occurrence of large-scale DNA fragmentation. Furthermore, pierisin-1 treatment caused ATM-independent Chk2 activation, suggesting the involvement of other kinases. At present, it is not clear how ATR or ATM sense DNA damages, such as bulky DNA adducts, and activate checkpoint responses. Most studies on checkpoint responses have been focused on DNA damage by physical sources, including IR and UV, and by chemical agents. Pieirisin-1 is a protein that mono-ADP-ribosylates specific sites in genomic DNA, so that it provides a unique tool to elucidate the effects of specific type of fork blockage on checkpoint activation and signaling.

Materials and Methods

Materials

Pierisin-1 was purified from pupae of *P. rapae* as described previously (2). Rabbit polyclonal antibodies to phospho-Chk1 (Ser^{345}) and phospho-Chk2 (Thr^{68}) and a mouse monoclonal antibody to phospho-ATM (Ser^{1981}) were purchased from Cell Signaling Technology, Inc. (Beverly, MA). A rabbit polyclonal antibody to Rad17 and a goat polyclonal antibody to ATR were obtained from Santa Cruz Biotechnology, Inc. (Santa Cruz, CA). A mouse monoclonal antibody to Chk2 and phosphorylated histone H2AX and a rabbit polyclonal antibody to phosphorylated histone H3 were purchased from Upstate Biotechnology (Charlottesville, VA). A goat polyclonal antibody to Chk1 and a mouse monoclonal antibody to ATM were from Bethyl Laboratory, Inc. (Montgomery, TX) and GeneTex, Inc. (San Antonio, TX), respectively. Horseradish peroxidase–conjugated secondary antibodies to rabbit and mouse IgG and to goat IgG were purchased from Amersham Biosciences Co. (Piscataway, NJ) and Santa Cruz Biotechnology, respectively. DNA polymerase α from calf thymus and DNA polymerase β from human were purchased from CHIMERx (Madison, WI). *Escherichia coli* DNA polymerase I and T4 polynucleotide kinase were from Takara (Otsu, Japan). All other chemicals were of the highest quality commercially available.

Cell Culture and Treatment

Human cervical carcinoma HeLa cells were obtained from the RIKEN Cell Bank (Tsukuba, Japan), transfected with a Bcl-2 expression vector (HeLa/Bcl-2) or a control vector, and maintained as described previously (12). $Rad17^{-/-}$ and $ATM^{-/-}$ DT40 cells were also established and maintained as detailed earlier (26, 38). ATM-deficient fibroblasts AT22IJE-T and a matched line complemented with an ATM minigene (ATM-deficient + ATM) were kindly provided by Dr. Yosef Shiloh (Tel Aviv University, Tel Aviv, Israel) and maintained in DMEM supplemented with 20% fetal bovine serum (21). The cells were incubated at 37°C in a humidified atmosphere containing 5% CO_2 and treated with various concentrations of pierisin-1 and other chemicals dissolved in DMSO for various times as indicated in each figure. Irradiation was carried out at the doses indicated using Gammacell ^{60}Co.

siRNA Transfection

Synthetic siRNA duplexes targeting ATM (AAGCGCCTGATTCGAGATCCT), ATR (AAGACGGTGTGCTCATGCGGC), Rad17 (AACAGACTGGGTTGACCCATC), and nonsilencing control (AATTCTCCGAACGTGTCACGT) were purchased from Qiagen Co. (Tokyo, Japan). HeLa cells were transfected with 100 nmol/L duplexes and Oligofectamine (Invitrogen, Tokyo, Japan) and analyzed 48 hours after transfection.

Preparation of an Oligonucleotide Template with ADP-Ribosylated Single Guanine Bases

A chemically synthesized 30-base oligonucleotide, 5′-CCAATCGCACACTTCTCCTCATTCCACTCA (10 μg), and 2 μg protease-activated pierisin-1 were incubated in 10 μL of 50 mmol/L Tris-HCl (pH 7.5), 2 mmol/L EDTA trisodium, and 1 mmol/L NAD for 24 hours at 37°C. The reaction mixture was subjected to high-performance liquid chromatography on TSK gel oligoDNA RP column (Tosoh, Tokyo, Japan) with the following elution system: linear gradient from 5% to 15% acetonitrile over 20 minutes in 0.1 mol/L ammonium acetate at

a flow rate of 1 mL/min. High-performance liquid chromatography analysis of a nuclease-digested mixture (8) of the separated oligonucleotides showed complete modification of a guanine base. In addition, urea-denatured PAGE-silver staining analysis showed that the high-performance liquid chromatography separation effectively removed oligonucleotide without ADP-ribosylation. The confirmed ADP-ribosylated oligonucleotide was used as a template for the following studies.

Polymerase Arrest Assay

For 5′-end labeling of the primer, 14-base oligonucleotide 5′-TGAGTGGAATGAGG (200 ng) and 5 units T4 polynucleotide kinase were incubated in 10 μL of 1× T4 polynucleotide kinase buffer solution supplied by the manufacturer and 1 μCi [γ-^{32}P]ATP (25 Ci/mmol) for 60 minutes at 37°C, and the enzyme was inactivated at 70°C for 5 minutes. Next, the labeled 14-base oligonucleotide (100 ng) and the 30-base oligonucleotide (1 μg), either ADP-ribosylated or unmodified, were annealed for primer extension study. The annealed DNA (40 ng template + 4 ng labeled primer) and various DNA polymerase were incubated in 2 μL of 50 mmol/L Tris-HCl (pH 8.0), 5 mmol/L $MgCl_2$, 0.02% bovine serum albumin, 1 mmol/L DTT, 0.2 mmol/L spermidine, and 0.2 mmol/L each of dATP, dCTP, dGTP, and TTP. DNA polymerase α (0.2 unit), DNA polymerase β (0.05 unit), DNA polymerase I (0.05 unit), and HeLa cytosol (2 μg; prepared using Dounce homogenizer and ultracentrifuged after removing of nuclear fraction) were the enzyme sources in this study. To inhibit DNA polymerase α, 10 μg/mL aphidicolin was incubated in the reaction mixture. Reactions were terminated by addition of gel loading buffer containing formamide and heated at 95°C. Extension products were separated on 15% denaturing polyacrylamide gel and subjected to autoradiography.

Cell Cycle Analysis

For cell cycle distribution analysis, cells were fixed in 70% ethanol and stored at −20°C for >8 hours. Before sorting, cells were washed twice in PBS, resuspended in PBS supplemented with 0.5 μg/mL RNase A, and incubated for 30 minutes at room temperature. Cells were then stained in the same buffer supplemented with 50 μg/mL propidium iodide, incubated for 1 hour at room temperature, and immediately analyzed using a FACSCalibur (Becton Dickinson, Franklin Lakes, NJ). Fluorescence data were displayed as peaks using the CellQuest software (Becton Dickinson). For quantitation of phosphorylated histone H3, cells were treated with pierisin-1 and nocodazole (50 ng/mL) for indicated time, and these cells were fixed, incubated with anti-phosphorylated histone H3 antibody (Upstate Biotechnology) and 1% bovine serum albumin/PBS for 2 hours at room temperature and with FITC-conjugated goat anti-rabbit antibody (Santa Cruz Biotechnology) for 1 hour at room temperature, and stained with propidium iodide for 1 hour at 37°C for fluorescence-activated cell sorting analysis.

DNA Synthesis Assay

Cells plated in 24-well culture dishes were transfected with siRNAs and labeled with 10 nCi/mL (specific activity, 50 mCi/mmol) [^{14}C]thymidine for 24 hours. Cells were then washed and incubated for 12 hours in nonradioactive medium. The cells were treated with or without pierisin-1 for 6 hours and then labeled with [^{3}H]thymidine (1 μCi/mL) for 15 minutes. At the end of the labeling period, the [^{3}H]thymidine-containing medium was removed, and the monolayers were fixed by addition of 5% trichloroacetic acid. The fixed cells were washed with thrice with trichloroacetic acid and then solubilized in 0.3 N NaOH. An aliquot of the NaOH-solubilized materials was transferred to a scintillation vial and neutralized by glacial acetic acid. After addition of scintillation fluid, incorporated [^{3}H]thymidine and [^{14}C]thymidine was measured by scintillation counting. The resulting ratio of ^{3}H to ^{14}C of a sample was presented as the percentage of the value of the untreated.

Colony Survival Assay

Clonogenic survival of wild-type, *Rad17*$^{-/-}$, and *ATM*$^{-/-}$ DT40 cells following pierisin-1 treatment at different concentration for 4 hours was determined. Serially diluted cells were plated in 60-mm dishes with 5 mL of 1.5% methylcellulose plates containing DMEM/F-12, 15% FCS, 1.5% chicken serum, penicillin/streptomycin, 2 mmol/L L-glutamine, and 10^{-5} mol/L β-mercaptoethanol after pierisin-1 treatment. Colonies were counted after 7 to 10 days and percentage survival was determined relative to the numbers of colonies from untreated cells.

Western Blot Analysis and Immunoprecipitation

After various treatments, cells were washed twice with ice-cold PBS and then lysed in radioimmunoprecipitation assay buffer [50 mmol/L Tris-HCl (pH 7.4), 150 mmol/L NaCl, 1% NP40, 0.25% sodium deoxycholate, 1 mmol/L Na_3VO_3, 1 mmol/L NaF, 1 mmol/L phenylmethylsulfonyl fluoride, 1 mmol/L EDTA] with protease inhibitor cocktail (Nacalaitesque, Tokyo, Japan) at 4°C for 15 minutes. The lysate was spun at 10,000 × *g* for 15 minutes at 4°C, and the supernatant was collected and stored at −80°C. Whole-cell lysates were then separated by SDS-PAGE and transferred onto polyvinylidene difluoride membranes for detection of proteins with antibodies. Horseradish peroxidase–conjugated IgG was used as the secondary antibody and specific immune complexes were visualized with the enhanced chemiluminescence detection system (Amersham Biosciences).

For immunoprecipitation experiments, whole-cell lysates were incubated with Chk1 antibody for overnight at 4°C, further incubated with protein G-Sepharose (Amersham Biosciences) for 1 hour at 4°C, and washed thrice with radioimmunoprecipitation assay buffer. Bound proteins were analyzed by SDS-PAGE followed by Western blotting.

Pulsed-Field Gel Electrophoresis

Levels of high molecular weight DNA fragmentation (1×10^5 cells per lane) were determined by using PFGE as reported previously (39). After various treatments, 1×10^5 cells in PBS were mixed with preheated (50°C), 2% low melting point agarose and transferred into agarose plug molds. After solidification at room temperature, the plugs were transferred into a solution containing 0.5 mol/L EDTA (pH 9.0), 1%

lauroylsarcosine, and 0.4 mg/mL proteinase K and incubated overnight at 50°C without agitation. Deproteinized DNA-containing agarose plugs were rinsed for period of 1 hour in 50 mmol/L EDTA (pH 8.0) buffer and stored until use at 4°C in the same buffer. Plugs were introduced into the 1% agarose gel and PFGE was carried out using a Clamped Homogeneous Controlled Electrodes Mapper System (Bio-Rad Laboratories, Inc., Hercules, CA). Fragments were separated at 14°C for 20 hours. Field strengths were 5.4 V/cm forward and 3.6 V/cm reverse, with initial and final switching times set 5 to 60 seconds with a liner ramp. Finally, gels were stained with ethidium bromide and visualized under UV light.

Acknowledgments

We thank Dr. Yosef Shiloh for providing ATM-deficient cells and a matched line complemented with an ATM minigene and Dr. Mami Takahashi and Cancer Prevention Basic Research Project and Biochemistry Division members for helpful discussion and critical reading of the article.

References

1. Koyama K, Wakabayashi K, Masutani M, et al. Presence in *Pieris rapae* of cytotoxic activity against human carcinoma cells. Jpn J Cancer Res 1996;87:1259–62.

2. Watanabe M, Kono T, Koyama K, Sugimura T, Wakabayashi K. Purification of pierisin, an inducer of apoptosis in human gastric carcinoma cells, from cabbage butterfly, *Pieris rapae*. Jpn J Cancer Res 1998;89:556–61.

3. Sugimura T. Serendipitous discoveries from sudden inspirations and the joy of being a scientist. Biochem Biophys Res Commun 2002;296:1037–8.

4. Kono T, Watanabe M, Koyama K, et al. Cytotoxic activity of pierisin, from the cabbage butterfly, *Pieris rapae*, in various human cancer cell lines. Cancer Lett 1999;137:75–81.

5. Kanazawa T, Watanabe M, Matsushima-Hibiya Y, et al. Distinct roles for the N- and C-terminal regions in the cytotoxicity of pierisin-1, a putative ADP-ribosylating toxin from cabbage butterfly, against mammalian cells. Proc Natl Acad Sci U S A 2001;98:2226–31.

6. Watanabe M, Kono T, Matsushima-Hibiya Y, et al. Molecular cloning of an apoptosis-inducing protein, pierisin, from cabbage butterfly: possible involvement of ADP-ribosylation in its activity. Proc Natl Acad Sci U S A 1999;96:10608–13.

7. Matsushima-Hibiya Y, Watanabe M, Hidari KI, et al. Identification of glycosphingolipid receptors for pierisin-1, a guanine-specific ADP-ribosylating toxin from the cabbage butterfly. J Biol Chem 2003;278:9972–8.

8. Takamura-Enya T, Watanabe M, Totsuka Y, et al. Mono(ADP-ribosyl)ation of 2′-deoxyguanosine residue in DNA by an apoptosis-inducing protein, pierisin-1, from cabbage butterfly. Proc Natl Acad Sci U S A 2001;98:12414–9.

9. Takamura-Enya T, Watanabe M, Koyama K, Sugimura T, Wakabayashi K. Mono(ADP-ribosyl)ation of the N^2 amino groups of guanine residues in DNA by pierisin-2, from the cabbage butterfly, *Pieris brassicae*. Biochem Biophys Res Commun 2004;323:579–82.

10. Totsuka Y, Kawanishi M, Nishigaki R, et al. Analysis of HPRT and supF mutations caused by pierisin-1, a guanine specific ADP-ribosylating toxin derived from the cabbage butterfly. Chem Res Toxicol 2003;16:945–52.

11. Shiotani B, Watanabe M, Totsuka Y, Sugimura T, Wakabayashi K. Involvement of nucleotide excision repair (NER) system in repair of mono ADP-ribosylated dG adducts produced by pierisin-1, a cytotoxic protein from cabbage butterfly. Mutat Res 2005;572:150–5.

12. Kanazawa T, Kono T, Watanabe M, et al. Bcl-2 blocks apoptosis caused by pierisin-1, a guanine-specific ADP-ribosylating toxin from the cabbage butterfly. Biochem Biophys Res Commun 2002;296:20–5.

13. Zhou BB, Elledge SJ. The DNA damage response: putting checkpoints in perspective. Nature 2000;408:433–9.

14. Zhou BB, Bartek J. Targeting the checkpoint kinases: chemosensitization versus chemoprotection. Nat Rev Cancer 2004;4:216–25.

15. Li L, Zou L. Sensing, signaling, and responding to DNA damage: organization of the checkpoint pathways in mammalian cells. J Cell Biochem 2005;94:298–306.

16. Belguise-Valladier P, Fuchs RP. *N*-2-aminofluorene and *N*-2 acetylamino-fluorene adducts: the local sequence context of an adduct and its chemical structure determine its replication properties. J Mol Biol 1995;249:903–13.

17. Ward IM, Minn K, Chen J. UV-induced ataxia-telangiectasia-mutated and Rad3-related (ATR) activation requires replication stress. J Biol Chem 2004;279:9677–80.

18. Zou L, Cortez D, Elledge SJ. Regulation of ATR substrate selection by Rad17-dependent loading of Rad9 complexes onto chromatin. Genes Dev 2002;16:198–208.

19. Guo N, Faller DV, Vaziri C. Carcinogen-induced S-phase arrest is Chk1 mediated and caffeine sensitive. Cell Growth Differ 2002;13:77–86.

20. Hotti A, Jarvinen K, Siivola P, Holtta E. Caspases and mitochondria in c-Myc-induced apoptosis: identification of ATM as a new target of caspases. Oncogene 2000;19:2354–62.

21. Ziv Y, Bar-Shira A, Pecker I, et al. Recombinant ATM protein complements the cellular A-T phenotype. Oncogene 1997;15:159–67.

22. Susin SA, Lorenzo HK, Zamzami N, et al. Molecular characterization of mitochondrial apoptosis-inducing factor. Nature 1999;397:441–6.

23. Wold MS. Replication protein A: a heterotrimeric, single-stranded DNA-binding protein required for eukaryotic DNA metabolism. Annu Rev Biochem 1997;66:61–92.

24. Zou L, Elledge SJ. Sensing DNA damage through ATRIP recognition of RPA-ssDNA complexes. Science 2003;300:1542–8.

25. Zou L, Liu D, Elledge SJ. Replication protein A-mediated recruitment and activation of Rad17 complexes. Proc Natl Acad Sci U S A 2003;100:13827–32.

26. Kobayashi M, Hirano A, Kumano T, et al. Critical role for chicken Rad17 and Rad9 in the cellular response to DNA damage and stalled DNA replication. Genes Cells 2004;9:291–303.

27. Bakkenist CJ, Kastan MB. DNA damage activates ATM through intermolecular autophosphorylation and dimer dissociation. Nature 2003;421:499–506.

28. Hirao A, Cheung A, Duncan G, et al. Chk2 is a tumor suppressor that regulates apoptosis in both an ataxia telangiectasia mutated (ATM)-dependent and an ATM-independent manner. Mol Cell Biol 2002;22:6521–32.

29. Takai H, Naka K, Okada Y, et al. Chk2-deficient mice exhibit radioresistance and defective p53-mediated transcription. EMBO J 2002;21:5195–205.

30. Jack MT, Woo RA, Hirao A, Cheung A, Mak TW, Lee PW. Chk2 is dispensable for p53-mediated G_1 arrest but is required for a latent p53-mediated apoptotic response. Proc Natl Acad Sci U S A 2002;99:9825–9.

31. Hirao A, Kong YY, Matsuoka S, et al. DNA damage-induced activation of p53 by the checkpoint kinase Chk2. Science 2000;287:1824–7.

32. Tsvetkov L, Xu X, Li J, Stern DF. Polo-like kinase 1 and Chk2 interact and co-localize to centrosomes and the midbody. J Biol Chem 2003;278:8468–75.

33. Bahassi el M, Conn CW, Myer DL, et al. Mammalian Polo-like kinase 3 (Plk3) is a multifunctional protein involved in stress response pathways. Oncogene 2002;21:6633–40.

34. Wei JH, Chou YF, Ou YH, et al. TTK/hMps1 participates in the regulation of DNA damage checkpoint response by phosphorylating CHK2 on threonine 68. J Biol Chem 2005;280:7748–57.

35. Saelens X, Festjens N, Vande Walle L, van Gurp M, van Loo G, Vandenabeele P. Toxic proteins released from mitochondria in cell death. Oncogene 2004;23:2861–74.

36. Yu SW, Wang H, Poitras MF, et al. Mediation of poly(ADP-ribose) polymerase-1-dependent cell death by apoptosis-inducing factor. Science 2002;297:259–63.

37. Ying W, Garnier P, Swanson RA. NAD^+ repletion prevents PARP-1-induced glycolytic blockade and cell death in cultured mouse astrocytes. Biochem Biophys Res Commun 2003;308:809–13.

38. Takao N, Kato H, Mori R, et al. Disruption of ATM in p53-null cells causes multiple functional abnormalities in cellular response to ionizing radiation. Oncogene 1999;18:7002–9.

39. Zhang X, Chen J, Graham SH, et al. Intranuclear localization of apoptosis-inducing factor (AIF) and large scale DNA fragmentation after traumatic brain injury in rats and in neuronal cultures exposed to peroxynitrite. J Neurochem 2002;82:181–91.

Molecular Cancer Research

Involvement of the ATR- and ATM-Dependent Checkpoint Responses in Cell Cycle Arrest Evoked by Pierisin-1

Bunsyo Shiotani, Masahiko Kobayashi, Masahiko Watanabe, et al.

Mol Cancer Res 2006;4:125-133.